Multiple Independent Comb Shaping (MICS): Phase-only generation of optical pulse sequences

Dmitry Pestov, Vadim V. Lozovoy, Marcos Dantus*

Department of Chemistry, Michigan State University, East Lansing, MI 48824
**dantus@msu.edu*

Abstract: A simple technique for the synthesis of optical pulse sequences is described, where the input laser spectrum is viewed as a superposition of independent but interlaced combs assigned to different sub-pulses. The devised concept enables intuitive programming of complex multi-pulse waveforms via one-dimensional phase-only shaping. Using this approach, we perform self-referenced cross-correlation measurements of various optical waveforms and demonstrate the generation and coding of shaped pulse sequences.

OCIS codes: (320.5540) Pulse shaping; (320.7100) Ultrafast measurements; (320.7160) Ultrafast technology.

References and links

1. D. J. Jones, S. A. Diddams, J. K. Ranka, A. Stentz, R. S. Windeler, J. L. Hall, and S. T. Cundiff, "Carrier-envelope phase control of femtosecond mode-locked lasers and direct optical frequency synthesis," Science **288**(5466), 635–639 (2000).
2. T. Udem, R. Holzwarth, and T. W. Hänsch, "Optical frequency metrology," Nature **416**(6877), 233–237 (2002).
3. Z. Jiang, C. B. Huang, D. E. Leaird, and A. M. Weiner, "Optical arbitrary waveform processing of more than 100 spectral comb lines," Nat. Photonics **1**(8), 463–467 (2007).
4. V. R. Supradeepa, C. B. Huang, D. E. Leaird, and A. M. Weiner, "Femtosecond pulse shaping in two dimensions: towards higher complexity optical waveforms," Opt. Express **16**(16), 11878–11887 (2008).
5. A typical ultrafast Ti:Sapphire laser oscillator, operating at 80 MHz and having 100-nm bandwidth, features about 10^6 comb lines within its spectrum. At the same time, the number of addressable pixels in a dispersive *4f* pulse shaper with a linear SLM in its Fourier plane ranges from 100 to ~1,000.
6. A. M. Weiner, and D. E. Leaird, "Generation of Terahertz-Rate Trains of Femtosecond Pulses by Phase-Only Filtering," Opt. Lett. **15**(1), 51–53 (1990).
7. M. M. Wefers, and K. A. Nelson, "Programmable Phase and Amplitude Femtosecond Pulse Shaping," Opt. Lett. **18**(23), 2032–2034 (1993).
8. A. M. Weiner, S. Oudin, D. E. Leaird, and D. H. Reitze, "Shaping of Femtosecond Pulses Using Phase-Only Filters Designed by Simulated Annealing," J. Opt. Soc. Am. A **10**(5), 1112–1120 (1993).
9. M. M. Wefers, and K. A. Nelson, "Generation of High-Fidelity Programmable Ultrafast Optical Wave-Forms," Opt. Lett. **20**(9), 1047–1049 (1995).
10. M. A. Dugan, J. X. Tull, and W. S. Warren, "High-resolution acousto-optic shaping of unamplified and amplified femtosecond laser pulses," J. Opt. Soc. Am. B **14**(9), 2348–2358 (1997).
11. T. Brixner, and G. Gerber, "Femtosecond polarization pulse shaping," Opt. Lett. **26**(8), 557–559 (2001).
12. D. Yelin, D. Meshulach, and Y. Silberberg, "Adaptive femtosecond pulse compression," Opt. Lett. **22**(23), 1793–1795 (1997).
13. T. Baumert, T. Brixner, V. Seyfried, M. Strehle, and G. Gerber, "Femtosecond pulse shaping by an evolutionary algorithm with feedback," Appl. Phys. B **65**(6), 779–782 (1997).
14. V. V. Lozovoy, I. Pastirk, and M. Dantus, "Multiphoton intrapulse interference. IV. Ultrashort laser pulse spectral phase characterization and compensation," Opt. Lett. **29**(7), 775–777 (2004).
15. B. W. Xu, J. M. Gunn, J. M. Dela Cruz, V. V. Lozovoy, and M. Dantus, "Quantitative investigation of the multiphoton intrapulse interference phase scan method for simultaneous phase measurement and compensation of femtosecond laser pulses," J. Opt. Soc. Am. B **23**(4), 750–759 (2006).
16. B. von Vacano, T. Buckup, and M. Motzkus, "In situ broadband pulse compression for multiphoton microscopy using a shaper-assisted collinear SPIDER," Opt. Lett. **31**(8), 1154–1156 (2006).
17. A. Galler, and T. Feurer, "Pulse shaper assisted short laser pulse characterization," Appl. Phys. B **90**(3-4), 427–430 (2008).
18. D. Meshulach, and Y. Silberberg, "Coherent quantum control of two-photon transitions by a femtosecond laser pulse," Nature **396**(6708), 239–242 (1998).
19. T. Brixner, N. H. Damrauer, P. Niklaus, and G. Gerber, "Photoselective adaptive femtosecond quantum control in the liquid phase," Nature **414**(6859), 57–60 (2001).

#112044 - $15.00 USD Received 28 May 2009; revised 9 Jul 2009; accepted 17 Jul 2009; published 31 Jul 2009

20. N. Dudovich, D. Oron, and Y. Silberberg, "Single-pulse coherently controlled nonlinear Raman spectroscopy and microscopy," Nature **418**(6897), 512–514 (2002).
21. T. Hornung, J. C. Vaughan, T. Feurer, and K. A. Nelson, "Degenerate four-wave mixing spectroscopy based on two-dimensional femtosecond pulse shaping," Opt. Lett. **29**(17), 2052–2054 (2004).
22. E. M. Grumstrup, S. H. Shim, M. A. Montgomery, N. H. Damrauer, and M. T. Zanni, "Facile collection of two-dimensional electronic spectra using femtosecond pulse-shaping Technology," Opt. Express **15**(25), 16681–16689 (2007).
23. J. C. Vaughan, T. Hornung, T. Feurer, and K. A. Nelson, "Diffraction-based femtosecond pulse shaping with a two-dimensional spatial light modulator," Opt. Lett. **30**(3), 323–325 (2005).
24. J. W. Wilson, P. Schlup, and R. A. Bartels, "Ultrafast phase and amplitude pulse shaping with a single, one-dimensional, high-resolution phase mask," Opt. Express **15**(14), 8979–8987 (2007).
25. E. Frumker, and Y. Silberberg, "Phase and amplitude pulse shaping with two-dimensional phase-only spatial light modulators," J. Opt. Soc. Am. B **24**(12), 2940–2947 (2007).
26. The experimental data reported in this work were partially presented at SPIE Photonics West 2009 (San Jose, CA - January 24–29, 2009)
27. A. M. Weiner, "Femtosecond pulse shaping using spatial light modulators," Rev. Sci. Instrum. **71**(5), 1929–1960 (2000).

1. Introduction

It is well-known that the spectrum of an ultrafast laser oscillator, firing a train of optical pulses, consists of closely spaced lines, referred to as a frequency comb. Phase-locking of comb lines for an over-octave laser spectrum has led to the Nobel Prize work on optical frequency metrology [1,2]. Phase and amplitude shaping of every line in that comb, in turn, would result in a universal laser source capable of truly arbitrary optical waveform generation, with exceptional fidelity. Such regime has been referred to as line-by-line shaping [3,4], as opposed to more conventional "group-of-lines" shaping when longitudinal laser modes are not resolved [5]. Ongoing developments in pulse shaping technology have enabled the generation of increasingly complex optical waveforms [3,4,6–11] and a variety of techniques for *in situ* laser pulse characterization and compression [12–17], poised to revolutionize photonics applications. Those applications include coherent control [18,19], simplifying multi-beam optical setups [20–22], or increasing the capacity of optical communication lines [3].

Pulse sequences, with controllable time delays and shapes, are an important class of optical waveforms. They are well suited for autocorrelation and cross-correlation measurements, pump-probe and some coherent control experiments, multidimensional and nonlinear spectroscopy such as photon echo and four-wave mixing. There has been an extensive amount of work on pulse train generation using a pulse shaper. Those efforts either utilize both phase and amplitude shaping (recreating the Fourier transform of the desired time-domain waveform) [7,17], mimic phase-and-amplitude modulation by means of diffraction in a phase-only shaper [23–25], or report on phase-only generation of pulse trains with fairly limited properties; see, e.g [6,8].

Here we present another strategy for pulse sequence synthesis, Multiple Independent Comb Shaping (MICS) [26]. Rather than trying to reconstruct the exact transfer function that shapes the input pulse into a desired pulse sequence, an approach that would require phase and amplitude modulation, we interlace the spectral phase functions for sub-pulses making up the pulse sequence and substitute the phase-and-amplitude modulation with a piecewise spectral phase mask. This intuitive concept streamlines multi-pulse waveform synthesis and enhances the capabilities of available pulse shaping instrumentation. In particular, we demonstrate how to use a one-dimensional phase-only shaper to generate groups of phase-modulated pulses, including double pulses for correlation measurements and multi-pulse waveforms for nonlinear optical experiments and communication lines.

Note that 'combs' in the discussion that follows are defined by the pulse shaper rather than by the repetition rate of the laser. Every comb 'tooth' may enclose, in principle, from one longitudinal mode of the laser cavity (line-by-line shaping) to many (group-of-lines shaping). We use those combs to sample the laser spectrum, build multiple replicas of the incoming laser pulse, and then shape/delay them to produce a desired pulse sequence.

The principle of MICS is illustrated in Fig. 1, where the synthesis of two independently controlled pulses is outlined. The laser spectrum is viewed as an interlay of two sub-combs,

#112044 - $15.00 USD Received 28 May 2009; revised 9 Jul 2009; accepted 17 Jul 2009; published 31 Jul 2009

each sampling the whole laser bandwidth. In the example shown, one comb is assigned a linear phase function corresponding to a time shift $-\tau$ of the slowly-varying field amplitude. The other has a cubic phase, centered at the carrier frequency ω_c. The resulting phase mask is a piecewise function defined across the entire laser spectrum. The approach is readily extendable to the generation of multi-pulse sequences. Interestingly, every pulse in such a train can be as short as the transform limit (TL) of the original spectrum; and it can be manipulated independently.

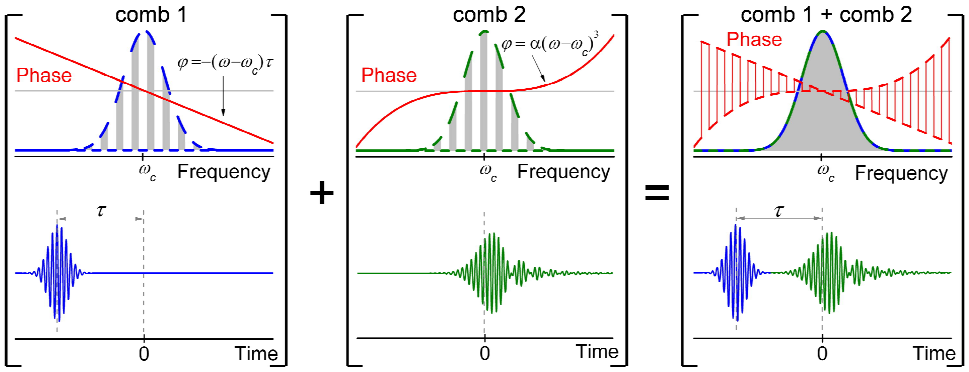

Fig. 1. The concept of multiple independent comb shaping (MICS). The sequence of two shaped pulses (e.g., a delayed TL pulse and a pulse with the third-order dispersion) is created by encoding a piecewise phase mask across the spectrum of an original TL laser pulse. This piecewise phase can be viewed as an alternating superposition of continuous phase functions applied to two independent subsets (combs) of the available spectrum.

2. Experimental

2.1. Experimental Setup

The layout of the experimental setup is shown schematically in Fig. 2. It includes a standard Ti:Sapphire laser oscillator (KMLabs, 86 MHz rep. rate, ~100-nm FWHM bandwidth) and a phase-only folded-4*f* pulse shaper [27] with a single-mask one-dimensional spatial light modulator (SLM-640-P, Cambridge Research & Instrumentation, Inc). The dispersed laser spectrum covered about 600 SLM pixels, with the resolution of 0.32 nm per pixel. The average precision of phase control for all wavelengths was 0.004 rad. While having the shaper calibrated within ± 2.5π from zero phase, we found it advantageous to work in the phase wrapping range between -π and + π; it reduced voltage variation and therefore minimized the cross-talk between pixels assigned to different combs. On the other hand, we did not bin pixels within a single comb tooth but rather adjusted their phase values in accordance with the programmed phase function, which was continuous for every particular comb. The time delay range, provided by the shaper, was ± 1.2 ps, as defined in Appendix A.

The output laser beam was attenuated and focused by a silver-coated mirror on a thin (~20 μm) KDP crystal, mounted on a glass slide. Second harmonic generation (SHG) in the nonlinear crystal, collected into a fiber-coupled spectrometer, was used as a feedback signal for pulse dispersion compensation via multiphoton intrapulse interference phase scan (MIIPS) [14,15] as well as for all other measurements discussed below. No mechanical delay lines were used to obtain the data presented.

#112044 - $15.00 USD Received 28 May 2009; revised 9 Jul 2009; accepted 17 Jul 2009; published 31 Jul 2009

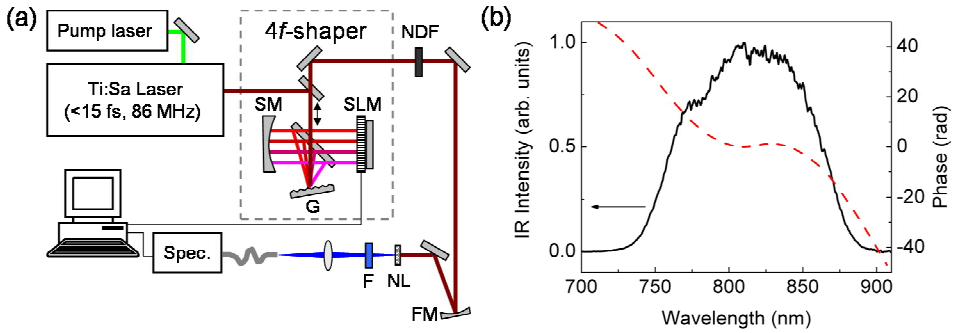

Fig. 2. (a) Layout of the experimental setup. G, plane-ruled grating (600/mm, Newport); SM, a 3-inch silver-coated spherical mirror (f = 500 mm, Thorlabs); SLM, spatial light modulator; NDF, neutral density filter; FM, focusing mirror (f = 250 mm); NL, nonlinear crystal; F, filter (BG39 glass); Spec., Ocean Optics S-2000 or USB4000 spectrometer. (b) Typical laser spectrum after the shaper (solid line) and MIIPS phase compensation mask (dashed line).

2.2. In situ autocorrelation and cross-correlation via phase-only shaping

We first demonstrate the capabilities of MICS as a means for obtaining auto- and cross-correlations. Spectrally-resolved non-background-free autocorrelation of a laser pulse can be attained by creating two pulse replicas, focusing the beam on a nonlinear crystal, and recording the SHG spectrum as a function of their time delay. One can keep the phase of the carrier-frequency mode fixed and shift only the envelopes of the two pulses to get non-background-free autocorrelation. Another option is to shift the envelope and the carrier-frequency phase simultaneously and acquire an interferometric autocorrelation trace, as one would have for a normal optical delay line and collinear beam geometry. Experimental spectrograms for the two cases are shown in Fig. 3(a). The corresponding autocorrelation curves, after integration over the SHG spectra, are given in Fig. 3(b). We refer to the two measurements as MICA and i-MICA, respectively. MICA stands for multiple-independent-comb assisted autocorrelation and emphasizes the fact that the pulse replicas used in these measurements is produced by MICS; for further details, see Appendix B.

Cross-correlation measurements of complex pulses with nonlinear phase modulation are presented in Fig. 3(c). We encode linear or quadratic chirp on one of the combs but keep the compensation mask for the second comb intact (TL reference), adding only the phase that shifts the pulse in time. Intensity-like multiple-independent-comb assisted cross-correlation (x-MICA) profile follows well the outline of the interferometric trace (xi-MICA) for the pulse with the third-order dispersion, when the effective carrier frequency is constant, but not so much for the linearly chirped pulse. This is because the non-interferometric measurements, MICA and x-MICA, are sensitive to the choice of the carrier frequency, which is required to calculate the pulse shaper phase masks. If the effective carrier frequency varies with time delay (as is the case, e.g., for a linearly chirped pulse) but one uses a fixed carrier frequency for the phase masks, MICA can no longer track the pulse envelope properly. We conclude that for complex waveforms, like the one shown at the bottom panel of Fig. 3(c), interferometric mapping via xi-MICA or i-MICA is preferred. Non-interferometric measurements, however, are still valuable for simple, close to TL waveforms. They can be performed much faster than interferometric ones because of the smaller number of experimental points needed.

The demonstrated phase-only cross-correlation reduces the burden on the shaper characteristics (no need for amplitude modulation) and also, e.g., allows for characterization of an amplified system output without jeopardizing its operation. When the pulse shaper is located between the oscillator and the regenerative amplifier, the amplified pulses can then be manipulated by this method without a concern of causing optical damage to components in the amplifier; see results obtained from this type of setup in Appendix C.

#112044 - $15.00 USD Received 28 May 2009; revised 9 Jul 2009; accepted 17 Jul 2009; published 31 Jul 2009

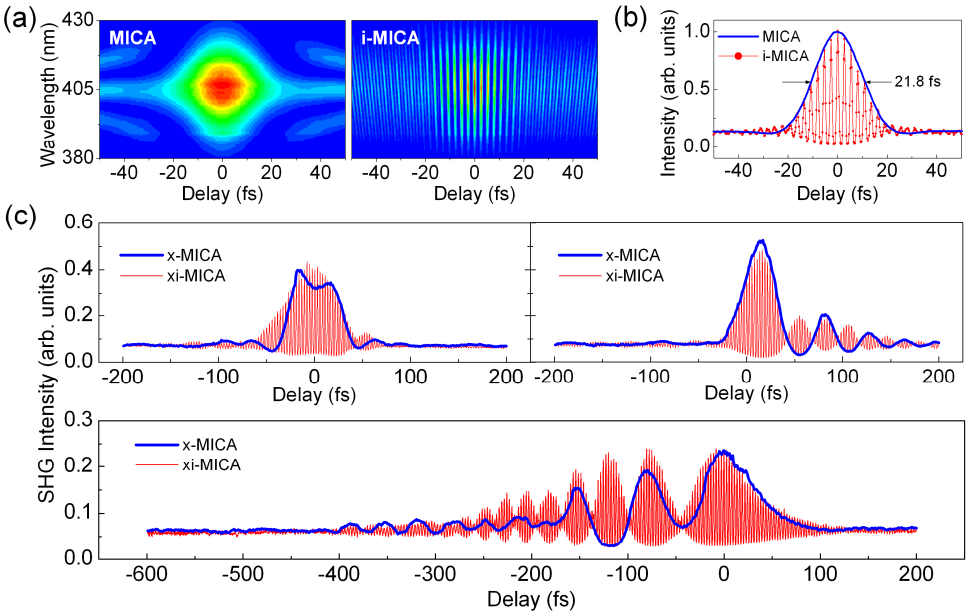

Fig. 3. Single-beam auto- and cross-correlation of optical waveforms via MICS. (a) Non-background-free and interferometric autocorrelation spectrograms (MICA and i-MICA, respectively) obtained experimentally for a TL 15-fs pulse. (b) Integrated SHG signal as a function of time delay between two pulse replicas. (c) Non-background-free and interferometric cross-correlation traces, x-MICA and xi-MICA, between a TL pulse and: (top-left) a pulse with the programmed second-order dispersion of + 300 fs^2; (top-right) a pulse with the programmed third-order dispersion of + 10,000 fs^3; (bottom) an original pulse right after the pulse shaper, with zero phase mask on the SLM. To obtain the TL pulse, MIIPS compensation mask is used.

2.3. Generation and coding of multi-pulse sequences

Figure 4 presents examples of more advanced MICS pulse trains. The piecewise phase mask in Fig. 4(a) produces a 3 + 1 pulse sequence that can be mapped by scanning the time delay of the fourth TL pulse. The resulting non-background-free cross-correlation spectrogram is shown in the inset of Fig. 4(b). The first pulse is programmed to have negative third-order dispersion; the second pulse has positive linear chirp; and the third pulse, at + 150 fs, is left TL. Note that while the optical waveform is fairly complex, the concept used to generate it is intuitive and simple. One can clearly see four overlaid phase functions corresponding to the four pulses of the programmed waveform. Their linear slopes (in the frequency domain) define the timing of the pulse envelopes within the sequence. The quadratic and cubic terms of combs 1 and 2 are responsible for the nonlinear phase distortions of the first two pulses. Comb 4 phase values are the only ones to be adjusted during the time delay scan. The interferometric cross-correlation trace in Fig. 4(b) is obtained for a similar pulse sequence but modeling a normal optical delay line. The linear phase terms for every comb then take zero value at $\omega = 0$, not the carrier frequency as shown in Fig. 4(a).

Finally, Fig. 4(c) demonstrates generation and coding of 6 + 1 pulse sequence, in the form suitable for optical communications. The sequence of six TL pulses is mapped by interferometric cross-correlation with the seventh TL pulse. Every comb is assigned about 86 pixels, 2 pixels per comb tooth. To remove a pulse from the sequence, the two pixels of every tooth in the corresponding spectral comb are assigned phases that differ by π. The π-step causes effective cancellation of the field within the pulse sequence time interval, distributing the associated energy outside the pulse shaper time range (or more generally, outside the time interval inversely proportional to the tooth spectral bandwidth). The average laser power

#112044 - $15.00 USD Received 28 May 2009; revised 9 Jul 2009; accepted 17 Jul 2009; published 31 Jul 2009

remains constant. Another similar way to eliminate a sub-pulse is to shift the phase by π for every other tooth of the corresponding comb; see Appendix D for details.

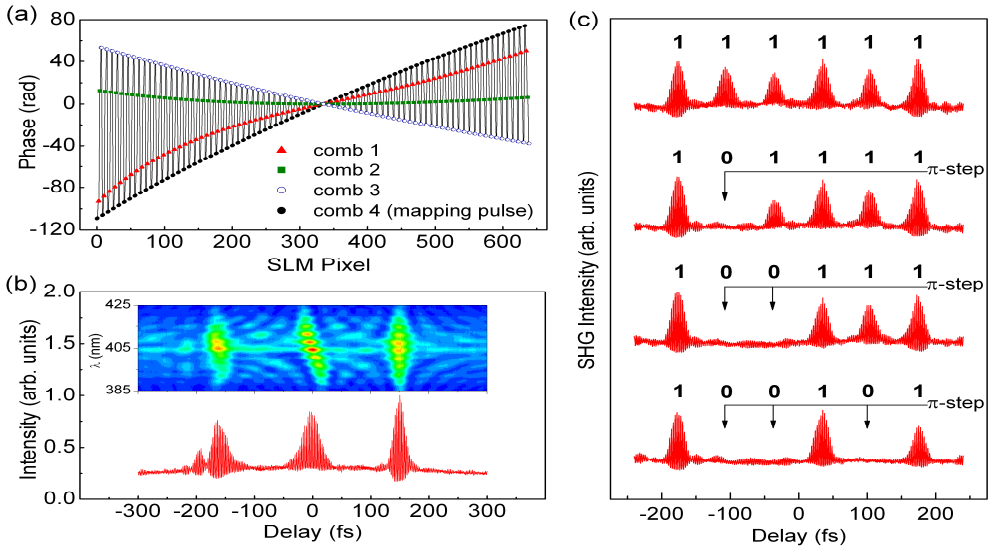

Fig. 4. MICS for generation and coding of multi-pulse sequences. (a) One of the unwrapped piecewise phase masks used to generate the x-MICA spectrogram, shown in the inset of Fig. 4(b). Pixel phase values that belong to the four combs are highlighted by different symbols. For the instance shown, the mapping pulse is delayed by −300 fs. (b) A 3 + 1 pulse sequence, with the first pulse having third-order dispersion of −5000 fs^3 (at −150 fs), the second pulse having the second-order dispersion of + 200 fs^2 (at 0 fs), and the third pulse being TL (at + 150 fs). The fourth pulse, also TL, is scanned from −300 fs to 300 fs to generate an interferometric cross-correlation trace. Two SLM pixels per peak are assigned for every comb. Inset: Non-background-free cross-correlation spectrogram of a similar pulse train but with the locked carrier frequency phase, when only pulse envelopes are shifted in time. (c) Multi-pulse generation and coding: the original 6 + 1 pulse sequence of 70-fs period, which corresponds to 14 THz rep. rate, is coded with π phase shifts that eliminate contributions of various pulses within the sequence. Two SLM pixels per tooth are assigned for every comb. For the pulse to be removed, the phase of one of the two pixels for every tooth in the corresponding comb is shifted by π.

2.4. 'Satellite' pulses

When the combs are designed by periodic sampling of the spectrum, 'satellite' peaks appear in the time domain, a consequence of not using amplitude modulation. Every spectral comb in this work is formed by a set of pixels, grouped in equidistantly spaced lines across the SLM mask; see the top panel in Fig. 5(a). Their structure can be then characterized by two parameters, δ and Δ, where δ is the tooth width, and Δ is the spacing between teeth in a comb. Their height is defined by the laser spectral intensity. The time interval between pulse replica's is then proportional to 1/Δ, while the scale at which they vanish is determined by 1/δ; here Δ and δ are to be expressed in frequency units. An example, where satellite pulses are prominent, is shown in Fig. 5(b). Note that because of limited spectral resolution of the shaper and slight aperiodicity of comb structure in the frequency domain, the attenuated copies of the pulse are distorted.

The chosen parameters (Δ/δ = 10) are meant to enhance the contribution of satellites. For a pair of identical pulses, as one has for MICA or i-MICA measurements, Δ/δ = 2 and the contribution of satellite field bursts into SHG is negligible; the peak-to-background ratio for a TL pulse in Fig. 3(b) is 8-to-1, as expected.

#112044 - $15.00 USD Received 28 May 2009; revised 9 Jul 2009; accepted 17 Jul 2009; published 31 Jul 2009

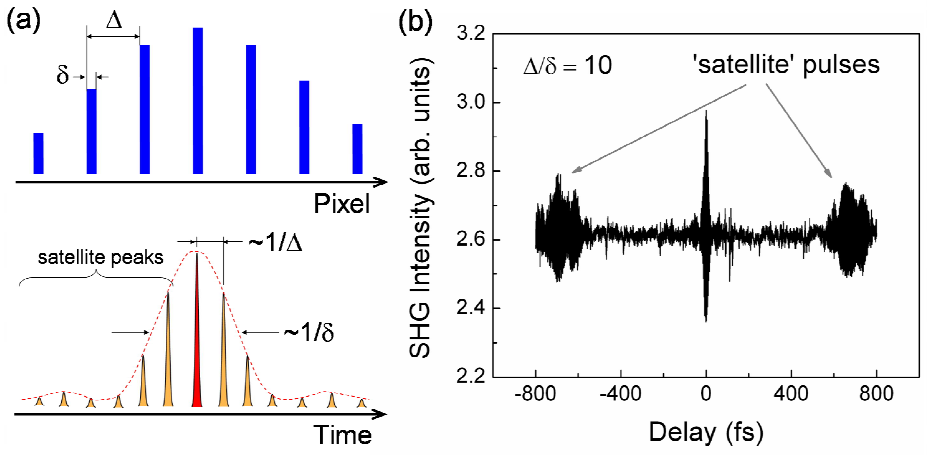

Fig. 5. (a) Spectral comb (top) and corresponding time domain structure (bottom) if the comb teeth are equidistantly spaced in the frequency domain. (b) Experimental xi-MICA profile between two unequal combs for Δ/δ = 10. Tooth width for the first comb is 1 pixel; the other has the tooth width of 9 SLM pixels.

When the laser spectrum is divided into N combs to synthesize a pulse sequence (see Fig. 6(a)), the peak amplitude of the measured SHG cross-correlation is proportional to $1/N^4$ (see Fig. 6(b)), as one would have for phase-and-amplitude modulation where the energy of every pulse scales as $1/N^2$ of the input energy. The contribution of satellite pulses into SHG can be deduced from the SHG 'background'. The obtained 'background' dependence on the number of combs suggests that a single spectral comb is equivalent to N pulses, each having $1/N^2$ of the total input energy; SHG signal is then proportional to $(1/N^2)^2 \times N^2$, i.e. $1/N^2$. The satellite pulses, however, do not contribute into the magnitude of cross-correlation peaks.

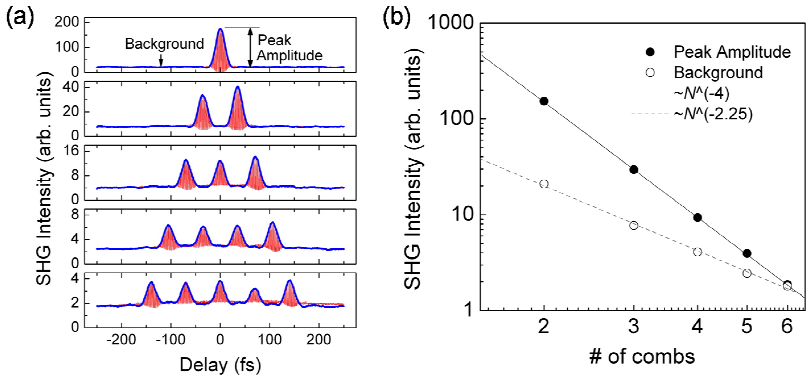

Fig. 6. (a) x-MICA and xi-MICA traces obtained for various-length pulse sequences, from 1 + 1 to 5 + 1, under fixed acquisition conditions. Two pixels per comb tooth are used for every pulse train. (b) Dependence of the acquired SHG intensity on the number of spectral combs in Fig. 6(a). When the scanned pulse does not overlap with any of the pulses in a sequence, collected SHG signal is referred to as background. The increase in the signal intensity due to the constructive interference of overlapped pulses is taken as peak amplitude. The experimental points are fitted with functions of the form $I_{SHG} = \alpha \cdot N^{\beta}$, where α and β are fitting parameters, and N is the number of combs.

#112044 - $15.00 USD Received 28 May 2009; revised 9 Jul 2009; accepted 17 Jul 2009; published 31 Jul 2009

3. Conclusions

We have presented a convenient basis for multi-pulse sequence synthesis. In such a basis, the spectral phase and/or amplitude masks, attributed to different sub-pulses, are decoupled while their interlaced spectral combs span the entire laser spectrum. Every pulse in the generated sequence can be as short as the input laser pulse and can be accessed and manipulated in a straightforward manner. As the first application of the devised MICS technique, we have demonstrated phase-only interferometric and non-interferometric cross-correlation of programmed optical waveforms, generation of shaped multi-pulse sequences, as well as their coding by means of binary phase shaping. Note that for MICA measurements to correlate with the standard auto- or cross- correlation traces, the spectral intensity and/or phase of the input pulse should not change significantly on the scale of comb period, i.e., they should be relatively smooth. One also needs to take into account the 'satellite' pulse contribution when the number of combs well exceeds two (generation of multiple pulses) or when the chosen comb tooth width is significantly larger than the spectral resolution of the shaper.

Acknowledgements

The authors would like to thank BioPhotonics Solutions, Inc. (Okemos, MI) for providing MIIPSBox software and a LabVIEW kit, which was used as a core of the developed user-shaper interface and automated data acquisition. They also acknowledge Xin Zhu who performed measurements on an amplified laser system. The data is shown in the Appendix C.

Appendix A: Shaper-assisted pulse delay range

The optical delay range that can be accessed through pulse shaping is defined entirely by the spectral resolution of the shaper. The reason is illustrated in Fig. A1. Every SLM pixel can be viewed as an independent channel that transmits the light within a narrow spectral window; see Fig. A1(a). The time duration of the optical waveform passing through a single pixel is large; however, when the pulses from several channels are recombined in phase at the shaper output, the ultrashort TL pulse is recreated; see the center panel in Fig. A1(a). The linear phase function, encoded on SLM, produces constructive interference between the channels at different time delay but does not shift the interfering waveform themselves. As a result, the created pulse follows their envelope, as shown at the bottom panel in Fig. A1(a).

The experimental curve in Fig. A1(b) defines the operating range of the shaper. The line is generated by scanning the slope of a linear phase function and recording the total intensity of the SHG signal. Enclosed MICA traces show that the pulse shape is preserved (time duration increases only by ~20% at the positive-delay end of the range) but its energy gets attenuated. The total IR power at the shaper output varies only by ±3.5% during such a scan.

If the optical beam spot size at the Fourier plane of the shaper is much smaller than the pixel size (bin size if the pixels are binned into groups), the light passing through a single channel has spectrum close to rectangular. The envelope of a single-channel waveform, therefore, has the following time-domain profile,

$$I = I_0 \times \left[\frac{\sin(\Delta\omega t / 2)}{\Delta\omega t / 2} \right]^2,$$

where $\Delta\omega$ is the spectral bandwidth of the channel. The position of the zero nodes is then equal to $\pm 2\pi n / \Delta\omega, n = 1, 2, 3, \ldots$. For the pulse shaper used in this work, calculations for binning 1, 2, 4, and 8 pixels at 800 nm give the node period of 6.6 ps, 3.3 ps, 1.7 ps, and 0.8 ps, respectively. These numbers converge with the experimental 4.7 ps, 2.9 ps, 1.5 ps, and 0.8 ps from Fig. A1(c), averaged over the recorded interval. In addition, slight increase of the oscillation period with the pulse delay can be seen in the experimental data.

#112044 - $15.00 USD Received 28 May 2009; revised 9 Jul 2009; accepted 17 Jul 2009; published 31 Jul 2009

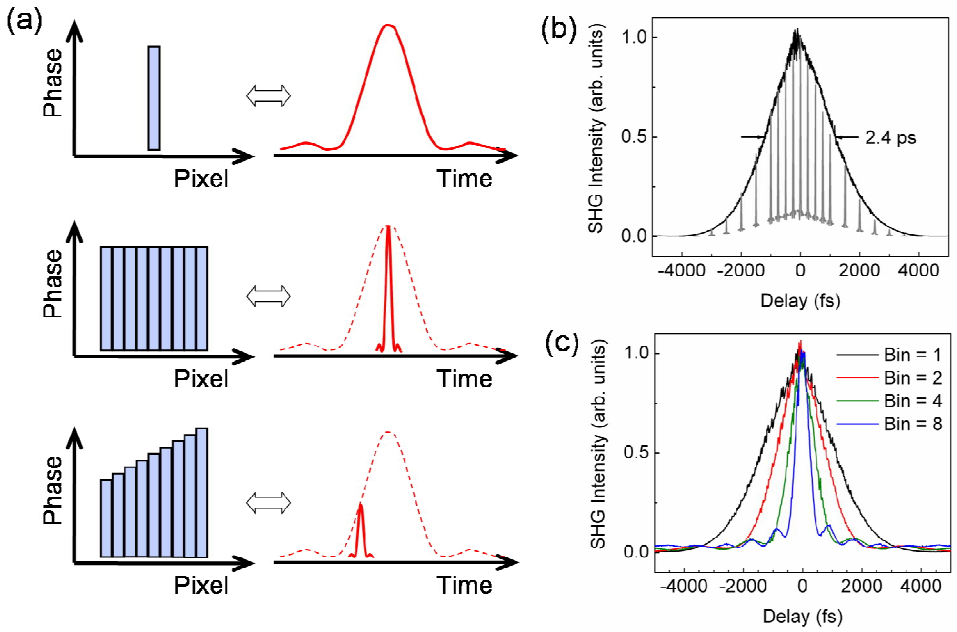

Fig. A1. Pulse shaper range. (a) Effect of shaper resolution on shaper-assisted time delay tuning: (top) single transmitting SLM pixel and corresponding optical waveform; (center) several transmitting SLM pixels and corresponding optical waveform at the shaper output. For simplicity, assume that the pixels are illuminated with equal intensity; (bottom) linear phase mask and its effect on the out-going laser pulse. (b) Pulse shaper range. Black line represents the total SHG signal as a function of time delay of a single TL pulse. The set of enclosed peaks (gray lines) are short-range MICA traces of the pulse for various time delays. (c) Total SHG signal as a function of the programmed time delay for different numbers of binned pixels. Binning is applied only to the linear phase function, not the phase distortion compensation mask.

Appendix B: MICA and i-MICA measurements

The difference between MICA and i-MICA procedures is presented schematically in Fig. A2. In case of MICA, the encoded linear phase function takes zero value at the chosen carrier frequency ω_c, i.e. it doesn't affect the field phase at ω_c. It causes the pulse envelope to shift in time but does not preserve its absolute phase; Fig. A2(a). In case of i-MICA (see Fig. A2(b)), the linear phase function crosses zero at $\omega = 0$. It shifts the pulse while keeping its absolute phase intact. This is exactly what one would have for a mechanical optical delay line.

#112044 - $15.00 USD Received 28 May 2009; revised 9 Jul 2009; accepted 17 Jul 2009; published 31 Jul 2009

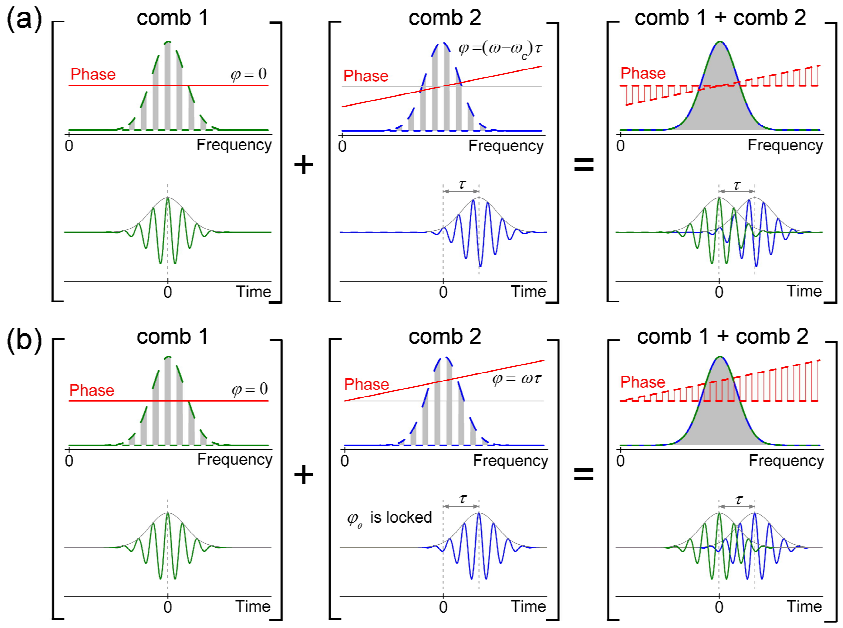

Fig. A2. Pulse self-characterization via MICS. (a) Pulse shaping for intensity-like multiple-independent-comb assisted autocorrelation (MICA). (b) Pulse shaping for interferometric multiple-independent-comb assisted autocorrelation (i-MICA).

Appendix C: Characterization of the amplifier output

We have also tested MICS-based pulse characterization on an amplified laser system, when a pulse shaper (MIIPSBox, BioPhotonics Solutions, Inc.) was set up in between the laser oscillator (KMLabs, Boulder) and a regenerative amplifier (Spitfire, Spectra Physics), as shown in Fig. A3(a). The linear one-dimensional SLM had 128 pixels (CRi SLM-128-P).

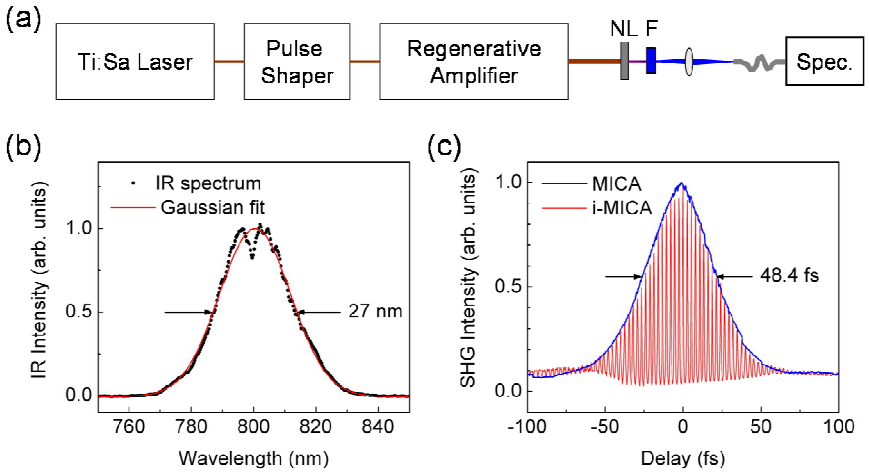

Fig. A3. Pulse characterization at the output of an amplified laser system. (a) Schematic diagram of the setup. NL, nonlinear crystal; F, color filter (BG39). (b) Output laser spectrum. (c) Experimental MICA and i-MICA traces. The autocorrelation FWHM corresponds to pulse duration of 34.2 fs.

#112044 - $15.00 USD Received 28 May 2009; revised 9 Jul 2009; accepted 17 Jul 2009; published 31 Jul 2009

Appendix D: Pulse sequence coding via binary shaping

There are at least two simple approaches to generate “0 states” in a given pulse train. In the first one, phase of every other pixel within a single comb tooth (and every tooth) is shifted by π relative to the phase of its neighbor, as depicted in Fig. A4(a). The implied assumption is that the comb teeth are assigned even number of SLM pixels (2 pixels in this case). The second approach is to add π to the phase of every other comb tooth; see Fig. A4(b). If the comb tooth width is similar (same number of pixels per tooth), the two approaches give almost the same result but with two minor points in favor of the second scheme. For the 3+1 pulse sequence in Fig. A4, the second approach gives better fidelity in cancellation of pulses 1 and 3. Also, binary shaping in the first scheme slightly affects the amplitude of other pulses. We believe both effects are due to more pronounced cross-talk between SLM pixels, when the first approach is used. Finally, the second technique imposes no restrictions on the number of SLM pixels per comb tooth; even one pixel per tooth suffices.

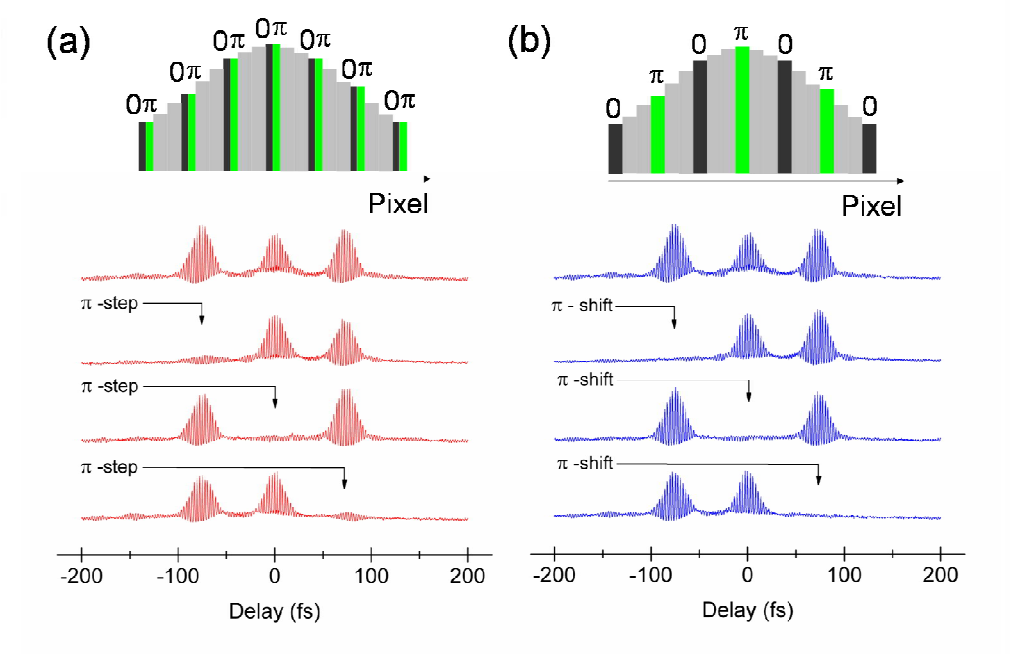

Fig. A4. Pulse sequence coding via binary shaping. (a) π-step is programmed on every 2-pixel comb tooth of the corresponding pulse. (b) π-shift is added to the phase of every other tooth in the comb.

#112044 - $15.00 USD Received 28 May 2009; revised 9 Jul 2009; accepted 17 Jul 2009; published 31 Jul 2009